Exploiting oxalotrophic bacteria to control *Aspergillus niger* lung infections

Short title: Bacteria-induced control of aspergillosis

Fabio Palmieri[1], Ilona Palmieri[1], Nourine Noormamode[1], Aislinn Estoppey[1], M. Omar Ishak[2], Julia M. Kelliher[2], Armelle Vallat[3], Rashi Iyer[4], Saskia Bindschedler[1], Karen Davenport[2], Patrick S. G. Chain[2], Jennifer Foster Harris[2], Pilar Junier[1]*.

[1] Laboratory of Microbiology, Institute of Biology, University of Neuchâtel, Neuchâtel, Switzerland.

[2] Bioscience Division, Los Alamos National Laboratory, Los Alamos, NM, USA.

[3] Neuchâtel Platform of Analytical Chemistry, University of Neuchâtel, Neuchâtel, Switzerland

[4] Analytics, Intelligence and Technology Division, Los Alamos National Laboratory, Los Alamos, NM, USA.

*Corresponding author

E-mail: pilar.junier@unine.ch (PJ)

Abstract

Fungal diseases are currently affecting a record number of people around the globe, with the genus *Aspergillus* representing one of the most prevalent groups of opportunistic fungal pathogens. Many aspects of the ecology of *Aspergillus* spp. are linked to pathogenicity, but so far, the ability to enhance their infectious potential by manipulating the environmental pH has not been considered. In this study we tested the hypothesis that by producing oxalic acid, *Aspergillus niger* can manipulate pH during lung infection and thus interfering with this process limits pathogenicity. To test this hypothesis, we co-cultured *A. niger* with bacteria that degrade oxalic acid (oxalotrophic bacteria) *in vitro*, as well as *ex vivo* using undifferentiated and differentiated lung cells in Transwells® inserts or bronchioles-on-a-chip systems. In the *in vitro* tests oxalotrophic bacteria suppressed the pH shift induced by *A. niger*, thereby effectively stopping growth. In *ex vivo* systems, *A. niger* also modified pH, Ca^{2+} and oxalic acid concentrations. Co-inoculation with as little as 10 cells of the oxalatrophic bacterium strongly inhibited the germination and development of *A. niger* and returned each of the three parameters to the baseline physiological values of uninfected cells. This offers the first demonstration of the use of oxalotrophic bacteria to control the growth of *A. niger* and represents a novel treatment paradigm that focuses on the manipulation of the environment as part of medical interventions to fight opportunistic fungal pathogens.

Authors summary

The rise of drug-resistant fungal infections is one of today's most imminent health risks for society. Despite the social and economic burden caused by infectious fungal diseases, this problem has been largely neglected. *Aspergillus* spp. is one of the most prevalent airborne opportunistic pathogens affecting human health. There are still significant gaps in our

knowledge surrounding its pathogenesis, as well as its interactions with host environmental factors, such as pH. In this study, we test the hypothesis that by producing oxalic acid, *Aspergillus niger* can manipulate pH during lung infection and thus interfering with this process limits pathogenicity. We showed the biocontrol potential of bacteria able to degrade oxalic acid (oxalotrophic bacteria) to control the growth of *A. niger in vitro* in Petri dishes, as well as in 3D-cell culture systems. Moreover, the coculture of oxalotrophic bacteria with *A. niger* permitted to return pH, Ca^{2+} and oxalic acid concentrations to the baseline physiological values of uninfected cells. In contrast to the traditional path of pathogen control by using antifungal agents, this offers the first demonstration of a novel treatment paradigm in which the fungal pathogen is controlled by rendering the host environment less permissive for infection.

Introduction

Fungal diseases are estimated to kill more than 1.5 million people every year, with the number of affected patients expected to increase even further [1,2]. Indeed, over the last three decades, the intensification in the burden of fungal disease on human health has correlated with an increase in the number of individuals from at-risk populations [3]. As the size of these populations (for instance, immunosuppressed patients) is expected to keep increasing in the future [2], tackling fungal pathogenesis is urgent. However, only a very limited number of antifungal drugs is used nowadays to control fungal pathogens. Because of this restricted chemical arsenal, the same classes of molecules are used in human health, animal husbandry, and agriculture, leading to the rise, and rapid spread, of resistance in fungal pathogens that can affect both plant and animal hosts [4]. In spite of this, tackling fungal disease has been largely neglected [5].

66 The most prevalent fungal pathogens affecting humans are airborne opportunists such as
67 *Aspergillus* spp., *Cryptococcus* spp., *Pneumocystis* spp., and human-associated commensals
68 like *Candida albicans* [6,7]. These fungal species are responsible for approximately 90% of the
69 deaths due to fungal infection [1]. The ecology of all these organisms plays a very significant
70 role in their ability to transition from harmless to pathogenic. A good example of this is the
71 genus *Aspergillus*, whose members are widespread in the environment and are commonly
72 isolated from both the outdoor and indoor environments [8,9]. The remarkable plasticity in the
73 ecology and stress-response of *Aspergillus* spp. is believed to form the basis of its success as
74 an opportunistic pathogen [9]. Indeed, species from this genus, and in particular *Aspergillus*
75 *fumigatus*, are thought to cause about 450'000 deaths worldwide every year [5].

76 Although many aspects of the ecology of *Aspergillus* spp. have been connected to pathogenicity
77 (e.g. nutritional plasticity, reproductive success, and tolerance to environmental stressors), the
78 ability to manipulate pH via the secretion of low molecular weight organic acids, and in
79 particular, oxalic acid, has been largely ignored in the context of human pathogenesis. Several
80 clinical reports have shown the presence of calcium oxalate crystals in pulmonary aspergillosis
81 in animals and humans [10–15]. Oxalic acid and oxalate crystals are thought to directly cause
82 damage to the host tissues (including pulmonary blood vessels), and to generate free radicals
83 which can harm cells indirectly [14]. A recent case report of invasive pulmonary aspergillosis
84 in a 69-year old man with lymphoma and pneumonia indicated the presence of calcium oxalate
85 crystals around blood vessels and within the blood vessel walls. This suggests a potential
86 mechanical role of oxalate crystals in the angioinvasion of *Aspergillus* [15]. However, a link
87 between oxalic acid production and pathogenicity has not yet been made in fungi from this
88 genus or in any other fungal human pathogen; despite having been widely acknowledged in the
89 case of fungal plant pathogens, where pH manipulation by the secretion of oxalic acid plays a
90 direct role in pathogenesis [16–18]. Acidification of the local environment is exploited by plant

91 pathogens to weaken the cell wall structure, facilitate infection, inhibit plant defenses, and
92 induce programmed cell death [17,19].

93 Oxalic acid is an ubiquitous compound in the environment. Its production and consumption by
94 microorganisms have been directly associated with pH regulation in soil [20]. In such
95 ecosystems, oxalic acid is often found complexed with divalent cations, especially calcium [21].
96 Despite its chemical stability (K_{sp} calcium oxalate monohydrate = 2.32×10^{-9}), calcium oxalate
97 rarely accumulates [22,23]. This is because calcium oxalate is used by soil oxalotrophic bacteria
98 as both a carbon and energy source. The transformation of a strong organic acid into a weaker
99 one (oxalic acid versus carbonic acid; pK_a = 1.25 and 4.14, respectively), creates a local
100 increase in soil pH [24].

101 We hypothesize that oxalic acid production may be needed for *Aspergillus* spp. to manipulate
102 pH during lung infection and that interfering with this process may limit pathogenicity. Such
103 intervention can be accomplished in two different ways. One method is to interfere with the
104 ability of the fungus to produce oxalic acid, for instance by knocking out one or more essential
105 genes in the synthesis pathway. Although valid under laboratory conditions, this option cannot
106 be considered for a therapeutic intervention. The second approach could aim at reducing the
107 concentration of oxalic acid *in situ* by directly removing this compound. This can be achieved
108 by using oxalotrophic bacteria. This approach offers an alternative that can be envisioned for a
109 future therapeutic intervention, based on the manipulation of the lung microbiota (Fig. 1).
110 Therefore, we chose to investigate this second alternative in order to offer a proof-of-concept
111 of the potential of using oxalotrophic bacteria to control the course of fungal pathogenesis.

112 To test our hypothesis, we selected *Aspergillus niger* as a model. This organism has been
113 extensively studied for its ability to produce oxalic acid [25,26] and is a known agent of
114 aspergillosis in humans [9]. We first confirmed that *A. niger* secretes oxalic acid and measured

115 the effect of co-cultivation with oxalotrophic bacteria *in vitro*. Then, we investigated the impact
116 of co-cultivation on human bronchial epithelial cells (HBEC) cultures where we determined a
117 dose-response effect for both the fungus and the bacteria. Finally, we used Transwells® inserts
118 and bronchioles-on-a-chip (BoC) systems to measure the effect of the fungus and the co-
119 cultivation with an oxalotrophic bacterium on pH, calcium concentration, oxalic acid
120 concentration, and tissue integrity.

121

122 ## Results

123 **Detection of oxalic acid produced by *Aspergillus niger* in different culture conditions**

124 Since the metabolism of fungi can change significantly depending on the nutritional conditions
125 of the growth medium, we first tested whether the strain of *A. niger* used for the experiments
126 produces oxalic acid on different standard laboratory media. Ultra-High Performance Liquid
127 Chromatography (UHPLC) analysis confirmed that the fungus produced oxalic acid as the sole
128 low molecular weight organic acid when grown in malt and in Reasoner's 2 liquid media (Fig.
129 S1A). Acidification and the presence of calcium oxalate crystals could also be detected upon
130 growth in water yeast agar (WYA) (Fig. S1B). We thus concluded that *A. niger* consistently
131 produced oxalic acid and acidified its medium under laboratory growth conditions.

132

133 **Confrontation assays between *A. niger* and selected bacterial strains**

134 We proceeded to test how the presence of oxalotrophic bacteria impacts the growth of *A. niger*
135 and the evolution of the pH in different growth media. Two oxalotrophic bacteria (*Cupriavidus*
136 *necator* and C. *oxalaticus*) and one non-oxalotrophic bacterium (*Pseudomonas putida*) were
137 used in confrontation assays. In malt agar diluted 10 times (MA 1/10), *A. niger* colonized the

138 entire Petri dish, including the area in which the bacterial inocula were applied. All the three
139 bacteria inoculated did not survive in the area of interaction with the fungus (Fig. S2A). In
140 Reasoner's 2 agar (R2A), *A. niger* did not colonize the area beyond the barrier formed by the
141 bacterial inoculum, but some microcolonies formed in the co-culture with *P. putida* beyond the
142 bacterial inoculation zone (Fig. S2B). In water yeast agar (WYA), fungal growth was also
143 restricted to the area delimited by the inocula in the co-culture with the two oxalotrophic
144 bacteria, while *P. putida* did not survive the interaction with the fungus, which instead,
145 colonized the entire plate. Moreover, in WYA medium, which contained a pH indicator, the
146 acidification of the medium by the fungus grown alone or in co-culture with the non-
147 oxalotrophic bacterium was clearly visible. In contrast, in the co-cultures with oxalotrophic
148 bacteria, the pH of the medium did not change (Fig. S2C). The control of fungal growth was
149 particularly remarkable in the case of *C. oxalaticus* (Fig. 2). The results in R2A and WYA
150 validate our hypothesis *in vitro* by demonstrating that fungal growth and pH can be controlled
151 by oxalotrophic bacteria.

152

153 **Growth tests in lung cells culture medium and confrontation assay between *A. niger* and**
154 ***C. oxalaticus***

155 In order to obtain evidence that oxalotrophic bacteria can control the growth of *A. niger* in a
156 lung infection model, we set up experiments on bronchial epithelial cell cultures. Given the
157 impact of the medium on the control of fungal growth, we repeated the growth and
158 confrontation assays in Air-Liquid Interface (ALI) medium, which is the medium used for
159 differentiation of lung cells [27]. The non-oxalotrophic bacterial model (*P. putida*) acidified the
160 medium after growth, while the oxalotrophic bacteria (*C. necator* and *C. oxalaticus*) did not
161 acidify the medium (Fig S3A). *C. oxalaticus* was found to also inhibit conidia germination and

162 mycelial development (Fig. S3B). Moreover, the presence of *C. oxalaticus* in co-culture with
163 the fungus stabilized the pH of the culture medium at a neutral pH (Fig. S3C), consistent with
164 decreased oxalic acid concentration in the medium (Fig. S3D). We therefore conclude that
165 oxalotrophic bacteria have a significant inhibitory effect on *A. niger* growth in ALI medium.

166

167 **Establishment of a dose-response curve on submerged cultures**

168 We established a dose-response curve for increasing conidial and/or bacterial loads on the
169 morphology of HBECs in submerged cultures. This aimed at identifying the optimal conidial
170 and/or bacterial load to perform additional experiments in Transwells® and BoC systems. After
171 24 hours, the overall size, shape and integrity of the lung cells changed at an absolute load of
172 500 conidia and above. The HBECs shrank in size due to actin agglomeration. Moreover, from
173 a conidial load of >=1000, fungal growth also had an adverse effect on tissue integrity (Fig.
174 S4). The same experiment was performed with *C. oxalaticus*. A strong morphological change
175 was induced by a total load of 500 bacterial cells and above. The HBECs became rounder, and
176 actin agglomeration increased compared with the cells-only control (Fig. S5). This indicates
177 that a dose of either 500 conidia or 500 bacterial cells is detrimental. To analyze the effect of
178 co-culturing *A. niger* with the oxalotrophic bacterium on HBECs integrity, we performed a test
179 with 10 and 500 conidia confronted with 10 bacterial cells. After 72h, *A. niger* induced
180 morphological changes (size reduction and actin agglomeration), with a stronger effect for 500
181 conidia, confirming the results obtained in the 24 h experiment. With the co-inoculation of as
182 few as 10 *C. oxalaticus* cells, the morphology of the HBECs was similar to the morphology of
183 HBECs of bacteria-only control, suggesting the inhibition of fungal development (Fig. S6). We
184 concluded that a conidial and bacterial load of 10 conidia/cells was ideal to monitor the

185 interaction of *A. niger* and *C. oxalaticus* in differentiated HBECs in Transwells® and BoC
186 systems.

187

188 **Biocontrol assay of *A. niger* bronchial cells infection by *C. oxalaticus***

189 After establishing a dose-response curve on HBECs in submerged cultures (Fig. S4-S6), the
190 effect of inoculation of 10 conidia of *A. niger* alone or in co-culture with 10 *C. oxalaticus* cells
191 was assessed in differentiated bronchial tissue in Transwells® inserts and BoC systems. In the
192 presence of the fungus alone, changes in three key environmental factors were observed: pH,
193 Ca^{2+} concentration, and concentration of soluble oxalic acid. The pH dropped significantly from
194 7.5 down to 4.5 in Transwells® and from 7.3 to 6.8 in BoC systems (Fig. 3A). Ca^{2+}
195 concentrations changed from 1 mM to around 0.2 mM in both culture systems (Fig. 3B). The
196 level of soluble oxalic acid dropped from 500 µM (cells alone) to 75 µM (cells inoculated with
197 the fungus) (Fig. 3C). pH, Ca^{2+} and free oxalic acid levels were statistically indistinguishable
198 when oxalotrophic bacteria were co-cultured with the fungus or in the controls with cells and
199 bacteria or cells alone. In addition, calcium oxalate crystals were observed in the cultures in
200 which the fungus developed (Fig. 3D), but not when the fungus was co-cultured with
201 oxalotrophic bacteria (Fig. 3E). This suggests that the lower levels of soluble oxalic acid
202 measured in the treatment with the fungus were likely the result of complexation of oxalic acid
203 and Ca^{2+} and corroborates the pH and Ca^{2+} concentration data. Moreover, the absence of
204 calcium oxalate crystals when the fungus was in co-culture with *C. oxalaticus* agrees with the
205 pH, Ca^{2+} concentration and soluble oxalic concentrations measured. These results validated our
206 hypothesis that oxalotrophic bacteria can be used to manipulate the microenvironment created
207 by *A. niger* and to hamper its development.

208 In addition to the changes in the environmental parameters measured above, we also observed
209 a cytopathic effect when conidia of *A. niger* developed into mycelia (Fig. 4A and B). The
210 absence of lactate dehydrogenase (LDH) activity measured in the medium in the treatment with
211 *A. niger* (Fig. 4C), supports the cytopathic effect and aggressiveness observed upon infection
212 by *A. niger*. LDH measurements were elevated in response to the presence of oxalotrophic
213 bacteria. Indeed, *C. oxalaticus* is a soil bacterium that is completely foreign to the lung
214 environment, thus potentially inducing an inflammatory response, something that needs to be
215 addressed for any future therapeutic application.

216

217 **Discussion**

218 By demonstrating the biocontrol activity that oxalotrophic bacteria exerted on *A. niger*, our
219 proof of concept study represents a novel paradigm in which the manipulation of the lung
220 environment is the focus of an anti-fungal medical intervention. This contrasts with the
221 prevailing use (and abuse) of antimicrobial compounds, which are instead directed to the
222 pathogen and inevitably result in the emergence of resistance [28]. To our knowledge, this is
223 the first demonstration of such an alternative approach for combatting human fungal infections
224 and is a significant step towards an integrated disease management strategy that is urgently
225 required to slow the emergence of resistance in fungal pathogens. Moreover, this approach can
226 be also relevant to *A. fumigatus*, the major causative agent of pulmonary aspergillosis, as the
227 presence of calcium oxalate crystals is reported in the literature, suggesting oxalic acid
228 production in this pathogen [8,11,14,29]. Currently there is an increasing interest in applying
229 ecological theory in lung microbiome research [30]. Although considered sterile for a long time,
230 the lung is now known to harbor a diverse microbiota [31,32]. In the healthy lung, this
231 microbiota is dominated by the genera *Prevotella*, *Streptococcus* and *Veillonella* [30,33]. Its

232 composition differs in a diseased state [34–36], and after transplantation [37]. Dysbiosis of the
233 lung microbiota associated with comorbidities in at-risk patients could make the lung
234 environment more permissive to fungal pathogens such as *Aspergillus* spp. This could in part
235 explain the current epidemic of nosocomial fungal infections [38]. Oxalate-degrading
236 capabilities have been previously reported in strains of the genera *Lactobacillus* [39],
237 *Streptococcus* [40], *Prevotella* [41,42] and *Veillonella* [42], all of which are represented in the
238 lung microbiota. In this context, assessing the oxalotrophic potential of the lung microbiome
239 and its subsequent stimulation could offer an endogenous alternative to fight aspergillosis.

240 Our results also provide an indication of additional roles of oxalic acid in fungal pathogenesis
241 in humans. Secretion of oxalic acid by the fungus has a clear effect on the concentration of free
242 Ca^{2+} in the medium. Calcium is known to be a secondary messenger in many cell types, playing
243 a central role in the activation of the immune response [43]. During immune stimulation, the
244 concentration of intracellular Ca^{2+} in immune cells increases thanks to Ca^{2+} entry from the
245 extracellular media or cellular compartments [44]. Accordingly, the use of a chelating agent of
246 divalent cations has been shown to inhibit the immune response *in vitro* [45,46]. This suggests
247 that chelation of Ca^{2+} in calcium oxalate crystals upon fungal infection could inhibit the immune
248 response. Moreover, the detection of calcium oxalate crystals is also meaningful in the case of
249 a chronic inflammatory response, as calcium oxalate crystals have been involved in
250 inflammation in renal cells [47]. A recent study also shows that calcium oxalate crystals induce
251 the production of inflammatory cytokines in primary and THP-1 monocytes [48]. Finally, a
252 recent study from McClintock *et al.* [49] showed the role of calcium in epithelial tissue cohesion
253 and barrier function, which could be disrupted upon fungal infection and subsequent Ca^{2+}
254 sequestration in the form of calcium oxalate.

255

256 ## Materials and Methods

257 ### Bacterial and Fungal cultures

258 All bacterial and fungal strains used in this study come from the collection of the Laboratory
259 of Microbiology of the University of Neuchâtel (LAMUN) and are summarized in Table 1. *P.*
260 *putida* KT2440 was kindly provided by Dr. Arnaud Dechesne (Technical University of
261 Denmark). *C. necator* JMP289 was kindly provided by Prof. Jan van der Meer (University of
262 Lausanne). *C. oxalaticus* Ox1 was tagged in-house using insertion with a MiniTn7 system.
263 Bacterial strains were routinely cultured on Nutrient Agar (NA, Carl Roth, Karlsruhe,
264 Germany) medium, whereas *Aspergillus niger* was routinely cultured on Malt Agar (MA)
265 medium. Potato Dextrose Agar (PDA, Carl Roth, Karlsruhe, Germany) was used for *A. niger*
266 conidia production. MA medium was composed of 12 g/L malt extract (Sios Homebrewing
267 GmbH, Wald, Switzerland) and 15 g/L agar (Biolife Italiana, Milano, Italy). Brain Heart
268 Infusion Agar (BHIA, Brain Heart Broth, Sigma-Aldrich, Darmstadt, Germany, 15 g/L agar)
269 was used to have mycelium-only colony edge without any conidia.

270

271 **Table 1. Bacterial and fungal strains used**

Code	Strain #	Species	Fluorescent tag	References
Pp	NEU 1264	*Pseudomonas putida* KT2440	GFP	[50]
Cn	NEU 1286	*Cupriavidus necator* JMP289	GFP	[51]
Co	NEU 1287	*Cupriavidus oxalaticus* Ox1	mCherry	[52]
An	NEU M8	*Aspergillus niger*	-	[53]

272 All the bacterial and fungal strains used in this study come from the collection of the Laboratory
273 of Microbiology of the University of Neuchâtel.

274

275 **Low Molecular Weight Organic Acids (LMWOA) detection by UHPLC and by**
276 **colorimetric pH indicator-based Petri dish assay**

277 In order to highlight the production of LMWOA by *A. niger*, we used Ultra-High-Performance
278 Liquid Chromatography (UHPLC), as well as a culture-based assay by using a pH indicator-
279 containing agar culture medium.

280 For the UHPLC analysis, 500 µl of 30 mM H_2SO_4 were added to 1 mL of a two-week liquid
281 culture in malt 1/10 and Reasoner's 2 liquid media in triplicate, to obtain 20 mM H_2SO_4 final
282 concentration. The samples were incubated at 60°C for two hours in order to dissolve
283 precipitated metal oxalate crystals, and then centrifuged at 3000 g for 10 min. All the samples
284 were filtered at 0.22 µm (13mm syringe filters, PTFE, hydrophilic) and 200 µl were added into
285 HPLC vials with 250 µl conical inserts. UHPLC (Ultimate 3000 RS-Dionex, Thermo Fisher
286 Scientific, MA, USA) was coupled with DAD detector set at 210 ± 2 nm. A 5 µL of sample
287 was injected onto a Prevail^{TM} organic acid column (5 µm particle size, 150 x 4.6 mm, Grace
288 Davison Discovery Sciences, Deerfield, IL, USA) with the temperature kept at 40°C. The
289 mobile phase consisted of 50 mM phosphate buffer adjusted to pH 2.5 with phosphoric acid
290 with a flow rate of 1 mL/min. Pure oxalic acid (Merck KGaA, Darmstadt, Germany) was
291 identified by the retention time and was quantified by an external standard curve, linear
292 regression from five calibration points (0.2 to 5 mg/mL).

293 For the culture-based assay, water yeast agar supplemented with bromocresol purple
294 (WYA+BP) [54] was used as a pH indicator-containing medium. WYP+BP was composed of
295 1 g K_2HPO_4, 5 g NaCl, 0.1 g yeast extract, 10 mg bromocresol purple and 20 g agar, per liter

296 of Milli-Q® water. After one week of incubation at room temperature, the presence of typical
297 bi-pyramidal shaped calcium oxalate crystals was assessed by observing a thin slice of agar
298 medium sampled at the edge of the colony and stained with lactophenol cotton blue under a
299 Leica DM4 B optical microscope connected to a Leica DFC7000 T camera.

300

301 **Confrontation assays on solid media**

302 Confrontations assays were performed between *A. niger* and three bacterial strains:
303 *Pseudomonas putida*, *Cupriavidus necator* and *Cupriavidus oxalaticus*, on three culture media
304 differing in their nutrient content. Malt agar diluted ten times (MA 1/10) was used as nutrient-
305 rich medium and was composed of 1.2 g/L malt extract (Sios Homebrewing GmbH, Wald,
306 Switzerland) and 15 g/L (Biolife Italiana, Milano, Italy). Reasoner's 2 agar (R2A) [55] was
307 used as nutrient-poor medium and the composition per liter of Milli-Q® water was the
308 following: 0.5 g yeast extract, 0.5 g Bacto Peptone, 0.5 g casamino acids, 0.5 g glucose, 0.5 g
309 soluble starch, 0.3 g Na-pyruvate, 0.3 g K_2HPO_4, 0.05 g $MgSO_4 \cdot 7H_2O$ and 15 g agar.
310 WYA+BP [54] was also used. *A. niger* was inoculated in the center of the plates containing the
311 different culture media. For that, a plug coming from the apical part of an active colony was
312 sampled using the wider end of a Pasteur pipette. The three different bacterial strains were
313 inoculated as opposite lines on either side of the fungal inoculum. Plates were incubated at
314 room temperature for 20 days, and pictures of the plates were taken. Pictures of the bacterial
315 inocula were taken using a Nikon SMZ18 epifluorescence stereoscope, connected to a Nikon
316 DS-Ri2 camera, in order to assess the viability of the bacterial strains thanks to constitutively
317 expressed fluorescent proteins.

318

319

320 **Growth tests and confrontation assay in Air-Liquid Interface (ALI) medium**

321 Air-Liquid Interface (ALI) medium was composed of DMEM/F12 (Cat.# 11320033, Thermo
322 Fisher Scientific) and LHC Basal Medium (Cat.# 12677019, Thermo Fisher Scientific) at a 1:1
323 ratio according to Fulcher *et al.* [27]. Bacterial growth in ALI medium was tested for 3 days at
324 room temperature. Increasing concentrations of Ca^{2+}, from 1 mM to 10 mM, was also tested on
325 bacterial and fungal growth in a 96-well plate. Given that ALI medium contains 1 mM Ca^{2+}, a
326 10 mM Ca^{2+} stock solution of ALI medium was prepared by adding 1.32 g/L $CaCl_2$ to have an
327 added Ca^{2+} concentration of 9 mM. This stock solution was used to prepare 8, 7.5, 6, 4.5, 3,
328 and 2.5 mM dilutions of $CaCl_2$ ALI-containing media. To produce fungal conidia, *A. niger* was
329 cultured on PDA for 10 days at room temperature. Conidia were then harvested by using
330 Dulbecco's Phosphate Buffer Saline (DPBS) supplemented with 0.01% (v/v) Tween 80.
331 Harvested conidia were washed tree times with DPBS following centrifugation at 2000xg for 5
332 min at room temperature. Finally, conidia were resuspended in 2 mL DPBS and quantified with
333 an Improved Neubauer counting chamber. Two µL of 1000 conidia/bacterial cell per µL
334 suspensions were inoculated in 200 µL ALI medium containing the Ca^{2+} concentrations
335 indicated above. To test mycelial growth in the different media, small agar plugs
336 (approximately 3 x 3 mm) coming from the edge of a colony of *A. niger* on BHIA were used.
337 The 96-well plate was incubated at room temperature for 7 days and growth was visually
338 assessed.

339 Confrontation of *A. niger* with *C. oxalaticus* was performed in 100-mm Corning® tissue culture
340 plate containing 12 mL ALI medium to allow the fungus to attach during growth. The fungal
341 inoculum was taken from the apical part of an active colony grown on BHIA by using the wider
342 end of a Pasteur pipette. For the confrontation assay, the fungal inoculum was placed in the
343 medium after addition and mixing of 100 µL inoculum of an overnight culture of *C. oxalaticus*
344 in ALI medium. A fungus-only plate was used as control. The plates were incubated at room

345 temperature for 7 days. Oxalic acid concentration was quantified by using the Oxalic Acid
346 Colorimetric Assay Kit (Sigma-Aldrich, Darmstadt, Germany, Cat.# MAK179), following the
347 manufacturer instructions.

348

349 **Preparation and sterilization of the bronchiole-on-a-chip (BoC)**

350 The chip was assembled as described in Hsieh, Nath and Huang [56]. Each unit of the culture
351 platform was fabricated by using a layer-by-layer stacking technique [57]. The devices were
352 designed using Solid Edge 2D software (ST9, Siemens PLM Software), and each layer of the
353 prelaminated polymeric sheet was obtained using a CO_2 laser cutter (Universal Laser System).
354 The prelaminated polymeric sheets were combined with biocompatible adhesive tapes (9122,
355 3M Company) with PMMA (1.5 and 3 mm thick) or PET (0.1 and 0.25mm thick). After cutting,
356 each layer was aligned and assembled using a seam roller to complete the devices. The culture
357 chip includes a Y-shaped apical and a basal part separated by a porous PET membrane (pore
358 size = 0.4μm) prepared as described in Arefin *et al.* [58]. The PET membrane was sandwiched
359 between two PET sheets using adhesive transfer tape to create the cell culture surface. This
360 allows nutrients to pass from the media to the cells through the porous membrane. The open
361 design of the tissue chip makes cell seeding procedure easy and accessible.

362 For sterilization, each chip was placed in a 100 mm Petri dish and sterilized with 5% hydrogen
363 peroxide solution for one hour. The chips were then rinsed 2-3 times with sterile deionized
364 water for 15 min between each rinse. Once all liquid was removed, the chips were let dry
365 overnight under a laminar flow hood. The next day, the inlet and outlet of the chip were
366 connected with a sterile tubing and rinsed 3 more times with sterile deionized water as explained
367 before. After the last rinse, 200 μl sterile DPBS was added in the channel (apical part) and 5
368 mL in the basolateral part (bottom part) of the chip, and the chip was placed in a humidified

369 incubator at 37°C with 5% CO_2 overnight. The next morning, peroxide contamination was
370 checked in each chip using a CG8+ i-STAT cartridge (Abbott, USA, Cat.# 03P88-25). Rinses
371 with sterile deionized water and overnight incubation with sterile DPBS were repeated until
372 peroxide was no longer detected in the devices.

373

374 **Primary normal human bronchial epithelial cell culture**

375 Primary normal human bronchial epithelial cells (Lifeline Cell Technology, Cat.# FC-0035)
376 were expanded in a T-75 cell culture flask with vent cap (Corning, Cat.# 3290) containing 13
377 mL BronchiaLife™ B/T complete medium (Lifeline Cell Technology, Cat.# LL-0023)
378 supplemented with 3 mL/L 0.5% Phenol Red solution (Sigma-Aldrich, Cat.# P0290, 15 mg/L
379 final concentration) to 70-80% confluence in a humidified incubator at 37°C with 5% CO_2.
380 Culture medium was changed every other day. Cells were used until passage 2 maximum for
381 all experiments. Cells were then harvested by trypsinization with 0.05% Trypsin / 0.02% EDTA
382 (Lifeline Cell Technology, Cat.# CM-0017), followed by the addition of Trypsin Neutralizing
383 buffer (Lifeline Cell Technology, Cat.# CM-0018), and counted using a hemocytometer after
384 centrifugation at 100xg for 5 min and resuspension of the cell pellet in BronchiaLife™ medium.

385 For submerged undifferentiated tissue culture in 96-well plates, 30'000 cells were seeded in
386 200 µl BronchiaLife™ medium per well. The 96-well plate was placed in a humidified
387 incubator at 37°C with 5% CO_2 for 2-3 days until confluence and formation of a monolayer of
388 bronchial cells.

389 For air-lifted differentiated tissue culture, Transwell® inserts in 24-well plates (Corning, Cat.#
390 3470) and BoC devices have first to be coated with collagen in order to allow proper cell
391 attachment onto the porous membrane. For that, 200 µL of 30 µg/mL rat collagen (Corning,
392 Cat.# 354236) diluted in DPBS were added to the apical side of Transwell® inserts and BoC

393 devices and the latter have been placed at 37 °C for 4 h in a 5% CO_2 humidified incubator.
394 Excess collagen was then removed, and all inserts and devices were rinsed once with sterile
395 DPBS and stored in a refrigerator until seeding of the cells.

396 Transwell® inserts and BoC devices were seeded on the apical side with 50'000 cells and
397 86'000 cells in 200 µL BronchiaLife™ complete medium, respectively. 600 µL of
398 BronchiaLife™ complete medium was added to the basolateral side of Transwell® inserts in
399 the 24-well plates and 3 mL in the basolateral side of the BoC device. All the inserts and device
400 were then placed in a humidified incubator at 37°C with 5% CO_2 for 2-3 days until confluence.
401 When bronchial cells formed a monolayer, they were shifted to air-liquid interface.
402 BronchiaLife™ complete medium was removed carefully from the apical part and replaced by
403 Air-Liquid Interface (ALI) Epithelial Differentiation Medium (Lifeline Cell Technology, Cat.#
404 LM-0050) supplemented with 3 mL/L 0.5% Phenol Red solution (Sigma-Aldrich, Cat.# P0290,
405 15 mg/L final concentration). The same was done for the medium in the basolateral side.
406 Finally, the medium on the apical side was removed and the inserts and devices were placed in
407 a humidified incubator at 37°C with 5% CO_2 for 21 days. Medium was changed every other
408 day as described previously. The cultures were observed daily using an EVOS™ XL Core
409 bright field inverted microscope (Thermo Fisher Scientific, CA, USA).

410

411 **Determination of conidial and bacterial load and confrontation assay on submerged**
412 **undifferentiated bronchial epithelial cell cultures**

413 In order to determine the optimal conidial and bacterial load to be used for confrontation on
414 bronchial tissue cultures, increasing conidial and bacterial loads were tested to assess their
415 effect on the morphology of bronchial epithelial cells in submerged cultures. *A. niger* was
416 cultured on PDA for 7 days at 37°C in order to produce conidia. *A. niger* conidia were then

417 harvested as already described. Finally, conidia were resuspended in 2 mL DPBS and quantified
418 with an Improved Neubauer counting chamber. Bacteria were cultured in BronchiaLife™
419 complete medium at 37°C overnight and quantified with an Improved Neubauer counting
420 chamber. A stock suspension of *A. niger* conidia was made at 1'000'000 conidia/mL that was
421 diluted further to obtain suspensions at 500'000, 100'000, 50'000, 10'000, 5000 and 1000
422 conidia/mL. The same was done for *C. oxalaticus* from a stock suspension at 100'000 bacterial
423 cells/mL diluted until 1000 bacterial cells/mL. 10 µL of each suspension was added to
424 submerged undifferentiated bronchial tissue in a 96-well plate in order to have 10'000, 5000,
425 1000, 500, 100, 50 and 10 conidia/well (200 µL) for *A. niger*, and 1000, 500, 100, 50, 10
426 bacterial cells/well (200 µL) for *C. oxalaticus*. The plates were placed in a humidified incubator
427 at 37°C with 5% CO_2 for 24h. For the confrontations assay, cells were infected with 10 or 500
428 *A. niger* conidia and were put in confrontation with 10 bacterial cells. Controls with only cells,
429 fungus or bacteria were also prepared. The plate was placed in a humidified incubator at 37°C
430 with 5% CO_2 for 72h.

431 After 24h or 72h incubation, the cells were fixed by adding 100 µL 4% paraformaldehyde in
432 DPBS per well and the plates were let sit for 15 min at room temperature. The cells were then
433 rinsed 3 times, with 2 min waiting time between each rinse. Two drops of ActinGreen™ 488
434 ReadyProbes™ Reagent (actin stain, Thermo Fisher Scientific, Cat.# R37110) and one drop of
435 NucBlue™ Live ReadyProbes™ Reagent (nuclei counterstain, Thermo Fisher Scientific, Cat.
436 # R37605) was added in 1 mL of DPBS to prepare the staining solution. 200 µL of staining
437 solution were added per well and the plates were let sit for 30 min at room temperature. Finally,
438 the cells were washed 3 times with DPBS before imaging with a Zeiss Axio Observer Z1
439 fluorescence inverted microscope (Carl Zeiss AG, Oberkochen, Germany).

440

441 **Confrontations on differentiated bronchial tissues in Transwell® inserts and BoC devices**

442 Differentiated bronchial tissues in Transwell® inserts and in BoC devices were infected with
443 10 µL of 1000 conidia or bacterial cell to get 10 conidia or bacterial cells. Fungus and bacteria
444 were co-inoculated for the confrontation and controls with only medium, cells, fungus or
445 bacteria were included. Each condition was done in triplicate for the Transwell® inserts and
446 one unique replicate for each condition was done for the BoC devices. All Transwell® inserts
447 and BoC devices were incubated in a humidified incubator at 37°C with 5% CO_2 for 72h.

448

449 **Immunofluorescence staining**

450 Differentiated bronchial tissues in Transwell® inserts and BoC devices were fixed by adding
451 100 µL 4% paraformaldehyde in DPBS per insert or device and the 24-well plate and devices
452 were let sit for 15 min at room temperature. The cells were then rinsed 3 times with 200 µL
453 DPBS, with 2 min waiting time between each rinse. Cells were permeabilized with 100 µL
454 0.5% Triton X-100 in DPBS for 15 min at room temperature and rinsed 3 times with 200 µL
455 DPBS, with 2 min waiting time between each rinse. After that, cells were blocked with 100 µL
456 3% BSA in DPBS for 1h at room temperature. Anti-Mucin 5AC mouse monoclonal antibody
457 (Abcam, Cat.# ab218466) was prepared in DPBS (1/100). The actin stain (ActinGreen™ 488
458 ReadyProbes™ Reagent, Thermo Fisher Scientific, Cat.# R37110) and the nuclei counterstain
459 (NucBlue™ Live ReadyProbes™ Reagent, Thermo Fisher Scientific, Cat. # R37605) were
460 added to the same buffer (2 drops/mL and 1 drop/mL, respectively). Anti-Aspergillus rabbit
461 polyclonal antibody (Abcam, Cat.# ab20419, RRID:AB_445571) was also added (1/200) in the
462 staining buffer for the conditions where *A. niger* conidia were inoculated. Fixed cells were
463 incubated with 100 µL buffer containing the stains and Anti-Mucin 5AC and Anti-Aspergillus
464 antibodies overnight at 4°C. The next day, fixed cells were washed 3 times with DPBS and

465 secondary antibodies were applied. Goat anti-Mouse IgG antibody (1/250) conjugated with
466 Alexa Fluor 546 (Thermo Fisher Scientific, Cat.# A-11003, RRID:AB_2534071) directed
467 against Anti-Mucin 5AC antibody and Goat anti-Rabbit IgG antibody (1/500) conjugated with
468 Alexa Fluor 594 (Thermo Fisher Scientific, Cat.# A-11012, RRID:AB_2534079) directed
469 against Anti-Aspergillus antibody were prepared in DPBS. Fixed cells were incubated with 100
470 µL buffer containing the secondary antibodies overnight at 4°C. The following day, fixed cells
471 were once again washed 3 times with DPBS and the membranes from the inserts were carefully
472 cut out with a sharp knife. The membranes were mounted on a glass slide using Fluoromount-
473 G™ Mounting Medium (Thermo Fisher Scientific, Cat.# 00-4958-02) and imaged with a Zeiss
474 Axio Observer Z1 fluorescence inverted microscope (Carl Zeiss AG, Oberkochen, Germany).

475

476 **pH measurements and quantification of calcium, oxalic acid and lactate dehydrogenase**
477 **(LDH)**

478 pH measurements of the culture medium after 72h incubation were done directly after taking
479 the samples out of the incubator using pH-indicator strips (Merck, Germany, Cat.# 109535) for
480 the Transwell® inserts samples, and CG8+ i-STAT cartridges (Abbott, USA, Cat.# 03P88-25)
481 for the BoC devices, as the pH change of the culture medium indicator was less visible. Free
482 calcium (Calcium Colorimetric Assay, Sigma-Aldrich, Darmstadt, Germany, Cat.# MAK022),
483 free oxalic acid (Oxalic Acid Colorimetric Assay Kit, Sigma-Aldrich, Darmstadt, Germany,
484 Cat.# MAK179), and LDH (ScienCell Research Laboratories, CA, USA, Cat. # 8078) were
485 quantified in the culture medium using colorimetric assay kits following the manufacturer
486 instructions.

487

488

489 **Statistical analyses**

490 Statistical significance of the data from the confrontations on differentiated bronchial tissues in
491 Transwell® inserts (3 replicates, n = 3) was tested with unpaired two-tailed Student t-tests in
492 Microsoft® Excel (Version 16.37). The statistical significance threshold was set to 5%.

Acknowledgments

We would like to thank Diego Gonzales and Ted Turlings for critical review of the paper, and Pulak Nath from the Materials Physics and Applications Division of the Los Alamos National Laboratory for providing the equipment and laboratory infrastructure for the BoC devices fabrication. BoC devices were developed under Defense Threat Reduction Agency (DTRA) interagency agreement CBMXCEL-XL1-2-0001. **Author contributions:** FP, PSC, JFH and PJ conceived and designed the study. FP, IP and NN performed the *in-vitro* experiments. AV performed the UHPLC analysis. FP performed the experiments related to cell work. JMK performed the microscopic observation of the CaOx crystals in the differentiated bronchial epithelial tissue. MOI fabricated and assembled the BoC devices. FP, JFH and PJ analyzed the data. FP and PJ wrote the paper, and all the authors reviewed and edited the paper. **Data and materials availability:** All data is available in the main text or the supplementary materials.

506 **References**

507 1. Fisher MC, Gurr SJ, Cuomo CA, Blehert DS, Jin H, Stukenbrock EH, et al. Threats Posed
508 by the Fungal Kingdom to Humans, Wildlife, and Agriculture. mBio. 2020/05/07 ed.
509 2020;11. doi:10.1128/mBio.00449-20

510 2. Bongomin F, Gago S, Oladele RO, Denning DW. Global and Multi-National Prevalence
511 of Fungal Diseases-Estimate Precision. J Fungi (Basel). 2018/01/27 ed. 2017;3.
512 doi:10.3390/jof3040057

513 3. Ramirez-Ortiz ZG, Means TK. The role of dendritic cells in the innate recognition of
514 pathogenic fungi (A. fumigatus, C. neoformans and C. albicans). Virulence. 2012/10/19
515 ed. 2012;3: 635–46. doi:10.4161/viru.22295

516 4. Fisher MC, Hawkins NJ, Sanglard D, Gurr SJ. Worldwide emergence of resistance to
517 antifungal drugs challenges human health and food security. Science. 2018/05/19 ed.
518 2018;360: 739–742. doi:10.1126/science.aap7999

519 5. Brown GD, Denning DW, Gow NAR, Levitz SM, Netea MG, White TC. Hidden Killers:
520 Human Fungal Infections. Science Translational Medicine. 2012;4: 165rv13.
521 doi:10.1126/scitranslmed.3004404

522 6. Brunke S, Mogavero S, Kasper L, Hube B. Virulence factors in fungal pathogens of man.
523 Curr Opin Microbiol. 2016/06/04 ed. 2016;32: 89–95. doi:10.1016/j.mib.2016.05.010

524 7. Pfaller MA, Diekema DJ. Rare and Emerging Opportunistic Fungal Pathogens: Concern
525 for Resistance beyond Candida albicans and Aspergillus fumigatus. Journal of Clinical
526 Microbiology. 2004;42: 4419–4431. doi:10.1128/jcm.42.10.4419-4431.2004

527 8. Kousha M, Tadi R, Soubani AO. Pulmonary aspergillosis: a clinical review. European
528 Respiratory Review. 2011;20: 156–174. doi:10.1183/09059180.00001011

529 9. Paulussen C, Hallsworth JE, Alvarez-Perez S, Nierman WC, Hamill PG, Blain D, et al.
530 Ecology of aspergillosis: insights into the pathogenic potency of Aspergillus fumigatus
531 and some other Aspergillus species. Microb Biotechnol. 2016/06/09 ed. 2017;10: 296–
532 322. doi:10.1111/1751-7915.12367

533 10. Kurrein F, Green GH, Rowles SL. Localized Deposition of Calcium Oxalate around a
534 Pulmonary Aspergillus niger Fungus Ball. American Journal of Clinical Pathology.
535 1975;64: 556–563. doi:10.1093/ajcp/64.4.556

536 11. Maeno T, Sasaki M, Shibue Y, Mimura K, Oka H. Calcium oxalate in the sputum may aid
537 in the diagnosis of pulmonary aspergillosis: A report of two cases. Med Mycol Case Rep.
538 2015/04/04 ed. 2015;8: 32–6. doi:10.1016/j.mmcr.2015.01.003

539 12. Muntz FH. Oxalate-producing pulmonary aspergillosis in an alpaca. Vet Pathol.
540 1999/11/24 ed. 1999;36: 631–2. doi:10.1354/vp.36-6-631

541 13. Oda M, Saraya T, Wakayama M, Shibuya K, Ogawa Y, Inui T, et al. Calcium oxalate
542 crystal deposition in a patient with Aspergilloma due to Aspergillus niger. J Thorac Dis.
543 2013/08/31 ed. 2013;5: E174-8. doi:10.3978/j.issn.2072-1439.2013.08.45

544 14. Payne CL, Dark MJ, Conway JA, Farina LL. A retrospective study of the prevalence of
545 calcium oxalate crystals in veterinary Aspergillus cases. J Vet Diagn Invest. 2016/11/18
546 ed. 2017;29: 51–58. doi:10.1177/1040638716672254

547 15. Yi Y, Cho SY, Lee DG, Jung JI, Park YJ, Lee KY. Invasive Pulmonary Aspergillosis Due
548 to Aspergillus awamori: Role of Calcium Oxalate Crystal Precipitation Mimicking
549 Mucormycosis. Mycopathologia. 2019/11/20 ed. 2019. doi:10.1007/s11046-019-00405-z

550 16. Lehner A, Meimoun P, Errakhi R, Madiona K, Barakate M, Bouteau F. Toxic and
551 signalling effects of oxalic acid. Canadian Journal of Microbiology. 2008;3: 746–748.
552 doi:10.1093/jxb/ern166.746

553 17. Dutton MV, Evans CS. Oxalate production by fungi: its role in pathogenicity and ecology
554 in the soil environment. Canadian Journal of Microbiology. 1996;42: 881–895.
555 doi:10.1139/m96-114

556 18. Palmieri F, Estoppey A, House GL, Lohberger A, Bindschedler S, Chain PSG, et al.
557 Oxalic acid, a molecule at the crossroads of bacterial-fungal interactions. Adv Appl
558 Microbiol. 2019/02/26 ed. 2019;106: 49–77. doi:10.1016/bs.aambs.2018.10.001

559 19. de Oliveira Ceita G, Macêdo JNA, Santos TB, Alemanno L, da Silva Gesteira A, Micheli
560 F, et al. Involvement of calcium oxalate degradation during programmed cell death in
561 Theobroma cacao tissues triggered by the hemibiotrophic fungus Moniliophthora
562 perniciosa. Plant Science. 2007;173: 106–117. doi:10.1016/j.plantsci.2007.04.006

563 20. Graustein WC, Cromack K Jr, Sollins P. Calcium oxalate: occurrence in soils and effect
564 on nutrient and geochemical cycles. Science (Washington, DC). 1977; 1252–1254.

565 21. Martin G, Guggiari M, Bravo D, Zopfi J, Cailleau G, Aragno M, et al. Fungi, bacteria and
566 soil pH: The oxalate-carbonate pathway as a model for metabolic interaction.
567 Environmental Microbiology. 2012;14: 2960–2970. doi:10.1111/j.1462-
568 2920.2012.02862.x

569 22. Hofmann BA, Bernasconi SM. Review of occurrences and carbon isotope geochemistry
570 of oxalate minerals: implications for the origin and fate of oxalate in diagenetic and
571 hydrothermal fluids. Chemical Geology. 1998;149: 127–146. doi:10.1016/S0009-
572 2541(98)00043-6

573 23. Certini G, Corti G, Ugolini FC. Vertical trends of oxalate concentration in two soils under
574 Abies alba from Tuscany (Italy). Journal of Plant Nutrition and Soil Science. 2000;163:
575 173–177. doi:10.1002/(SICI)1522-2624(200004)163:2<173::AID-JPLN173>3.0.CO;2-H

576 24. Braissant O, Cailleau G, Aragno M, Verrecchia EP. Biologically induced mineralization
577 in the tree Milicia excelsa (Moraceae): its causes and consequences to the environment.
578 Geobiology. 2004;2: 59–66. doi:10.1111/j.1472-4677.2004.00019.x

579 25. Ruijter GJG, van de Vondervoort PJI, Visser J. Oxalic acid production by Aspergillus
580 niger: an oxalate-non-producing mutant produces citric acid at pH 5 and in the presence
581 of manganese. Microbiology. 1999;145: 2569–2576. doi:10.1099/00221287-145-9-2569

582 26. Cameselle C, Bohlmann JT, Núñez MJ, Lema JM. Oxalic acid production by Aspergillus
583 niger. Bioprocess Engineering. 1998;19: 247–252. doi:10.1007/pl00009017

584 27. Fulcher ML, Gabriel S, Burns KA, Yankaskas JR, Randell SH. Well-Differentiated
585 Human Airway Epithelial Cell Cultures. In: Picot J, editor. Methods in Molecular
586 Medicine. 2005.

587 28. Toprak E, Veres A, Michel JB, Chait R, Hartl DL, Kishony R. Evolutionary paths to
588 antibiotic resistance under dynamically sustained drug selection. Nat Genet. 2011/12/20
589 ed. 2011;44: 101–5. doi:10.1038/ng.1034

590 29. Pabuççuoğlu U. Aspects of oxalosis associated with aspergillosis in pathology specimens.
591 Pathology Research and Practice. 2005;201: 363–368. doi:10.1016/j.prp.2005.03.005

592 30. Foesel BU, Pfeiffer S, Raj ACD, Etschmann SK, Schloter M. Applying ecological theories
593 in lung microbiome research: lessons learned from microbial ecology and evolution? In:
594 Cox MJ, Ege MJ, von Mutius E, editors. The Lung Microbiome. 2019. pp. 50–66.
595 doi:10.1183/2312508x.10015718

596 31. Enaud R, Prevel R, Ciarlo E, Beaufils F, Wieërs G, Guery B, et al. The Gut-Lung Axis in
597 Health and Respiratory Diseases: A Place for Inter-Organ and Inter-Kingdom Crosstalks.
598 Frontiers in Cellular and Infection Microbiology. 2020;10.
599 doi:10.3389/fcimb.2020.00009

600 32. Mitchell AB, Oliver BGG, Glanville AR. Translational Aspects of the Human Respiratory
601 Virome. American Journal of Respiratory and Critical Care Medicine. 2016;194: 1458–
602 1464. doi:10.1164/rccm.201606-1278CI

603 33. Charlson ES, Bittinger K, Haas AR, Fitzgerald AS, Frank I, Yadav A, et al. Topographical
604 Continuity of Bacterial Populations in the Healthy Human Respiratory Tract. American
605 Journal of Respiratory and Critical Care Medicine. 2011;184: 957–963.
606 doi:10.1164/rccm.201104-0655OC

607 34. Cui L, Lucht L, Tipton L, Rogers MB, Fitch A, Kessinger C, et al. Topographic Diversity
608 of the Respiratory Tract Mycobiome and Alteration in HIV and Lung Disease. American
609 Journal of Respiratory and Critical Care Medicine. 2015;191: 932–942.
610 doi:10.1164/rccm.201409-1583OC

611 35. Dickson RP, Martinez FJ, Huffnagle GB. The role of the microbiome in exacerbations of
612 chronic lung diseases. The Lancet. 2014;384: 691–702. doi:10.1016/S0140-
613 6736(14)61136-3

614 36. van Woerden HC, Gregory C, Brown R, Marchesi JR, Hoogendoorn B, Matthews IP.
615 Differences in fungi present in induced sputum samples from asthma patients and non-
616 atopic controls: a community based case control study. BMC Infectious Diseases.
617 2013;13: 69. doi:10.1186/1471-2334-13-69

618 37. Charlson ES, Diamond JM, Bittinger K, Fitzgerald AS, Yadav A, Haas AR, et al. Lung-
619 enriched Organisms and Aberrant Bacterial and Fungal Respiratory Microbiota after Lung
620 Transplant. American Journal of Respiratory and Critical Care Medicine. 2012;186: 536–
621 545. doi:10.1164/rccm.201204-0693OC

622 38. Suleyman G, Alangaden GJ. Nosocomial Fungal Infections: Epidemiology, Infection
623 Control, and Prevention. Infect Dis Clin North Am. 2016/11/07 ed. 2016;30: 1023–1052.
624 doi:10.1016/j.idc.2016.07.008

625 39. Turroni S, Vitali B, Bendazzoli C, Candela M, Gotti R, Federici F, et al. Oxalate
626 consumption by lactobacilli: Evaluation of oxalyl-CoA decarboxylase and formyl-CoA
627 transferase activity in Lactobacillus acidophilus. Journal of Applied Microbiology.
628 2007;103: 1600–1609. doi:10.1111/j.1365-2672.2007.03388.x

629 40. Miller A, Dearing D. The Metabolic and Ecological Interactions of Oxalate-Degrading
630 Bacteria in the Mammalian Gut. Pathogens. 2013;2: 636–652.
631 doi:10.3390/pathogens2040636

632 41. Ticinesi A, Nouvenne A, Chiussi G, Castaldo G, Guerra A, Meschi T. Calcium Oxalate
633 Nephrolithiasis and Gut Microbiota: Not just a Gut-Kidney Axis. A Nutritional
634 Perspective. Nutrients. 2020/02/26 ed. 2020;12. doi:10.3390/nu12020548

635 42. Suryavanshi MV, Bhute SS, Jadhav SD, Bhatia MS, Gune RP, Shouche YS.
636 Hyperoxaluria leads to dysbiosis and drives selective enrichment of oxalate metabolizing
637 bacterial species in recurrent kidney stone endures. Scientific Reports. 2016;6.
638 doi:10.1038/srep34712

639 43. Vig M, Kinet J-P. Calcium signaling in immune cells. Nature Immunology. 2009;10: 21–
640 27. doi:10.1038/ni.f.220

641 44. Grinstein S, Klip A. Calcium homeostasis and the activation of calcium channels in cells
642 of the immune system. Bull N Y Acad Med. 1989;65: 69–79.

643 45. Diamantstein T, Odenwald MV. Control of the immune response in vitro by calcium ions.
644 I. The antagonistic action of calcium ions on cell proliferation and on cell differentiation.
645 Immunology. 1974;27: 531–541.

646 46. Diamantstein T, Ulmer A. The control of immune response in vitro by Ca2+. II. The Ca2+-
647 dependent period during mitogenic stimulation. Immunology. 1975;28: 121–125.

648 47. Mulay SR, Kulkarni OP, Rupanagudi KV, Migliorini A, Darisipudi MN, Vilaysane A, et
649 al. Calcium oxalate crystals induce renal inflammation by NLRP3-mediated IL-1beta
650 secretion. J Clin Invest. 2012/12/12 ed. 2013;123: 236–46. doi:10.1172/JCI63679

651 48. Dominguez-Gutierrez PR, Kusmartsev S, Canales BK, Khan SR. Calcium Oxalate
652 Differentiates Human Monocytes Into Inflammatory M1 Macrophages. Front Immunol.
653 2018/09/07 ed. 2018;9: 1863. doi:10.3389/fimmu.2018.01863

654 49. McClintock SD, Attili D, Dame MK, Richter A, Silvestri SS, Berner MM, et al.
655 Differentiation of human colon tissue in culture: Effects of calcium on trans-epithelial
656 electrical resistance and tissue cohesive properties. Koval M, editor. PLoS ONE. 2020;15:
657 e0222058. doi:10.1371/journal.pone.0222058

658 50. Nelson KE, Weinel C, Paulsen IT, Dodson RJ, Hilbert H, Martins dos Santos VAP, et al.
659 Complete genome sequence and comparative analysis of the metabolically versatile
660 Pseudomonas putida KT2440. Environmental Microbiology. 2002;4: 799–808.
661 doi:10.1046/j.1462-2920.2002.00366.x

662 51. Sentchilo V, Czechowska K, Pradervand N, Minoia M, Miyazaki R, van der Meer JR.
663 Intracellular excision and reintegration dynamics of the ICEclc genomic island of

Pseudomonas knackmussii sp. strain B13. Mol Microbiol. 2009/05/13 ed. 2009;72: 1293–306. doi:10.1111/j.1365-2958.2009.06726.x

52. Şahin N, Işik K, Tamer AÜ, Goodfellow M. Taxonomic Position of "Pseudomonas oxalaticus" Strain Ox1T (DSM 1105T) (Khambata and Bhat, 1953) and its Description in the Genus Ralstonia as Ralstonia oxalatica comb. nov. Systematic and Applied Microbiology. 2000;23: 206–209. doi:10.1016/s0723-2020(00)80006-5

53. Ferro KI. The impact of oxalogenic plants on soil carbon dynamics - formation of a millennium carbon storage as calcium carbonate. Faculty of Sciences. University of Neuchâtel. 2012.

54. Mela F, Fritsche K, de Boer W, van Veen JA, de Graaff LH, van den Berg M, et al. Dual transcriptional profiling of a bacterial/fungal confrontation: Collimonas fungivorans versus Aspergillus niger. ISME J. 2011/05/27 ed. 2011;5: 1494–504. doi:10.1038/ismej.2011.29

55. Reasoner DJ, Geldreich EE. A new medium for the enumeration and subculture of bacteria from potable water. Applied and Environmental Microbiology. 1985;49: 1.

56. Hsieh H-L, Nath P, Huang J-H. Multistep Fluidic Control Network toward the Automated Generation of Organ-on-a-Chip. ACS Biomaterials Science & Engineering. 2019;5: 4852–4860. doi:10.1021/acsbiomaterials.9b00912

57. Lin CK, Hsiao YY, Nath P, Huang JH. Aerosol delivery into small anatomical airway model through spontaneous engineered breathing. Biomicrofluidics. 2019/08/14 ed. 2019;13: 044109. doi:10.1063/1.5121188

58. Arefin A, McCulloch Q, Martinez R, Martin SA, Singh R, Ishak OM, et al. Micromachining of Polyurethane Membranes for Tissue Engineering Applications. ACS Biomaterials Science & Engineering. 2018;4: 3522–3533. doi:10.1021/acsbiomaterials.8b00578

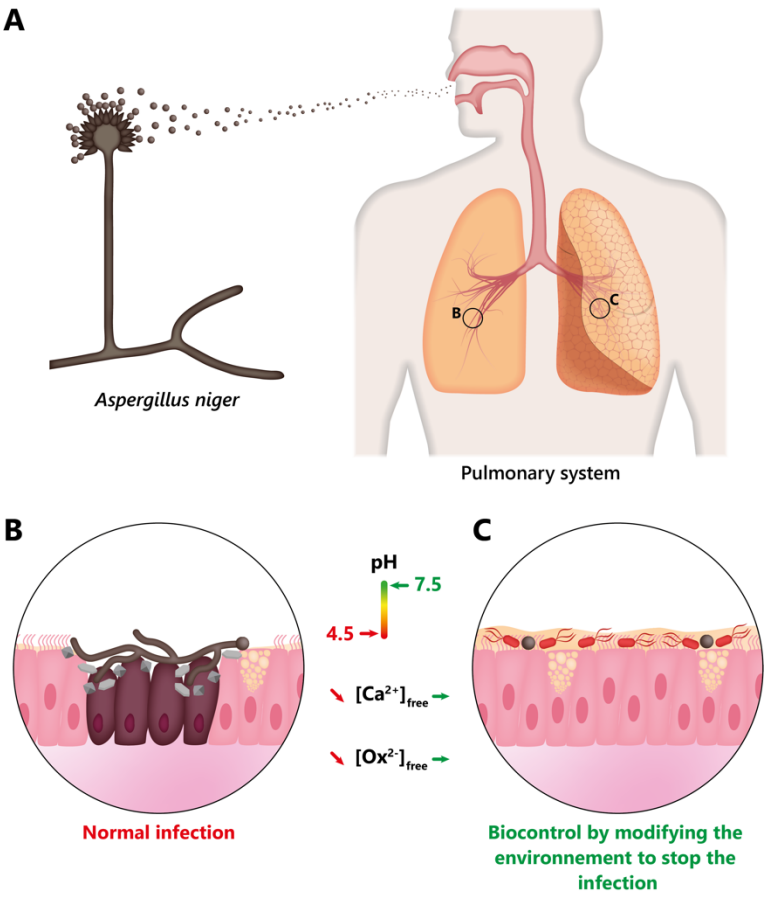

690

691 **Fig. 1. Schematic summary of the proposed strategy to control *Aspergillus niger* infection**
692 **by introducing oxalotrophic bacteria to modify the *A. niger* environmental niche.** (A) *A.*
693 *niger* conidia (depicted in dark grey) arrive in the respiratory system through breathing. (B)
694 During a normal infection process in a susceptible host, *A. niger* modifies the environment by
695 secreting oxalic acid (or oxalate Ox^{2-}) which decreases pH and chelates free calcium in the form
696 of calcium oxalate (CaOx; depicted in light grey) crystals. This results in the infection of the
697 host's tissue. (C) The biocontrol strategy proposed here takes advantage of the ability of
698 oxalotrophic bacteria (cells depicted in red) to consume CaOx and thus reestablish
699 physiological pH and free calcium concentrations.

700

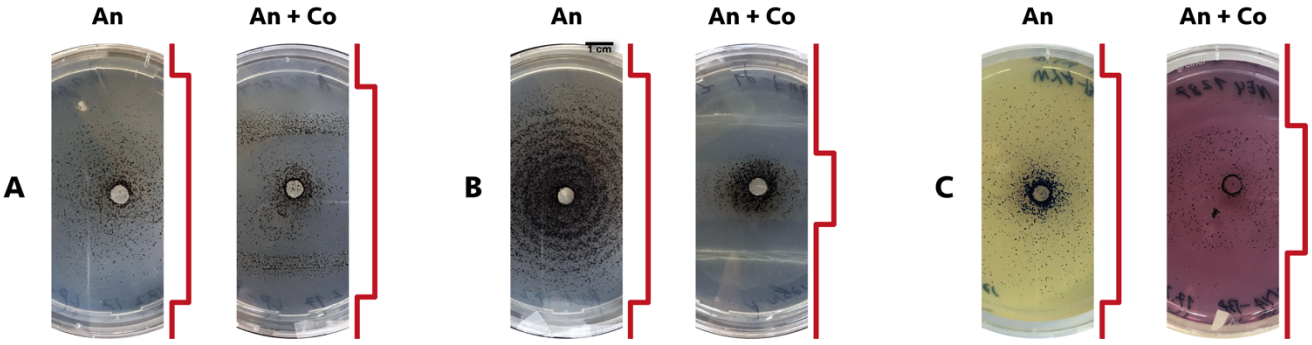

Fig. 2. Comparison of the growth of *Aspergillus niger* (An) alone and in confrontation with *Cupriavidus oxalaticus* (Co) in different culture media. The red line next to each picture represents the extent of *A. niger* growth. On MA 1/10 (A), there is no significant growth inhibition of *A. niger*, as it kills *C. oxalaticus*. *A. niger* growth is highly restricted to the center of the plate when co-cultured with *C. oxalaticus* on R2A (B). The growth inhibition of *A. niger* when co-cultured with *C. oxalaticus* is less pronounced on WYA + BP (C).

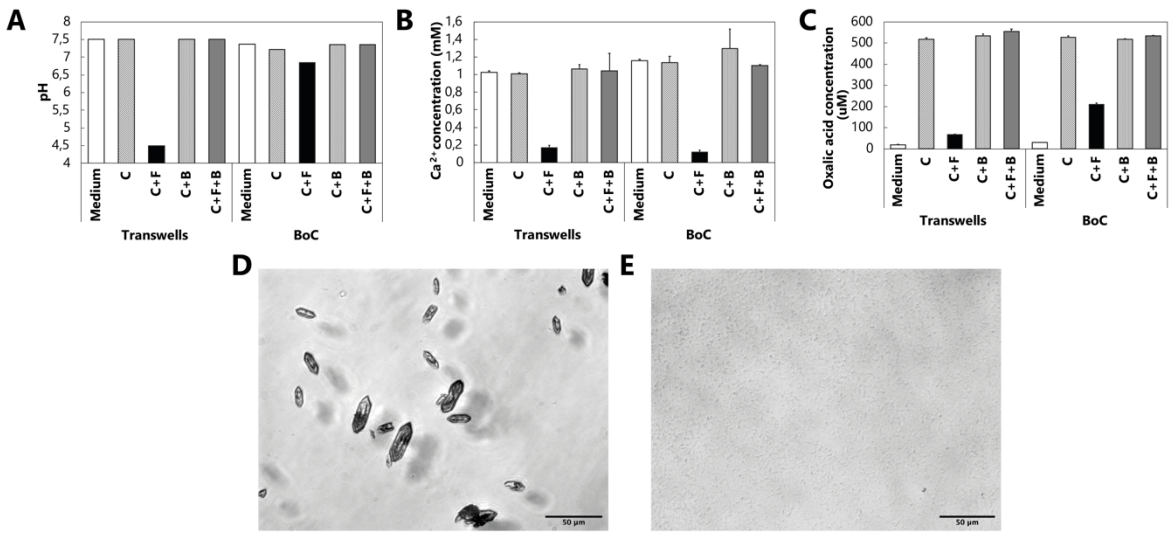

Fig. 3. Influence of the interaction between *Aspergillus niger* and the oxalotrophic bacterium *Cupriavidus oxalaticus* on environmental parameters of differentiated bronchial tissue in Transwell® inserts and bronchiole-on-a-chip (BoC) devices. In the presence of the fungus, the pH (A) decreases, as compared to all other treatments. This pH decrease is correlated with a drastic decrease in the concentration of free Ca^{2+} (B) (*p*-value between C and C+F = $8{,}951 \times 10^{-7}$**)**. Free oxalic acid concentrations were lower in the presence of the fungus, compared with the basal level secreted by the bronchial cells (C) (*p*-value between C and C+F = $4{,}587 \times 10^{-8}$**)**. These results are supported by the detection of calcium oxalate crystals in the presence of the fungus (D). In the co-culture with the oxalotrophic bacterium, pH, free Ca^{2+} and free oxalic acid concentrations return to physiological levels, and this was concomitant with the absence of crystals (E) (*p*-values between C+F and C+F+B for free Ca^{2+} and free oxalic acid = 0,002 and $1{,}415 \times 10^{-7}$, respectively). C: lung cells; C+F: lung cells + fungus; C+B: lung cells + bacteria; C+F+B: lung cells + fungus + bacteria. For A, B, C, the results represent the mean + sd of three independent measurements for the Transwell® inserts for each condition (three biological replicates, n = 3). For A, pH results for the BoC devices represent a unique measurement per condition (one replicate, n = 1). For B and C, Ca^{2+}

726 and oxalic acid results for the BoC devices represents the mean + sd of two measurements per

727 condition (one replicate).

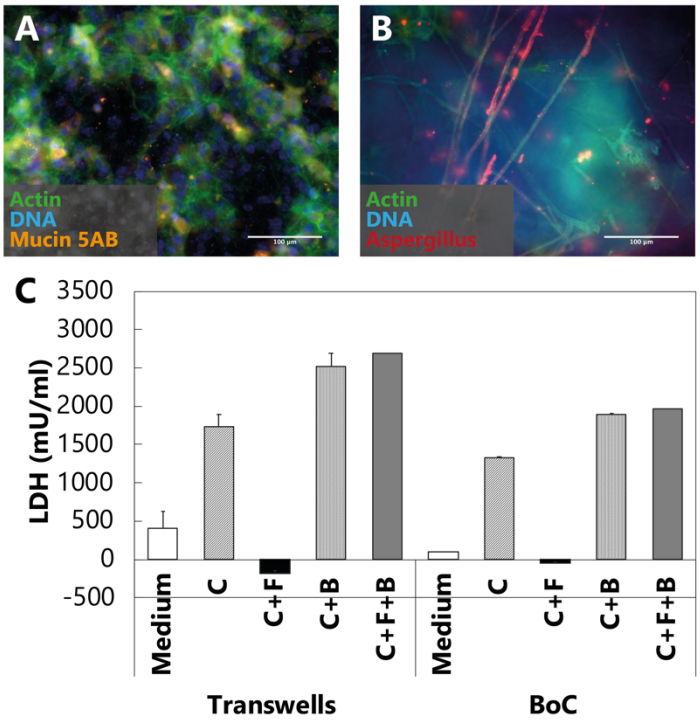

728

729 **Fig. 4. Cytopathic effect of *Aspergillus niger* on differentiated bronchial tissue and lactate**
730 **dehydrogenase (LDH) measurements of the co-culture between *A. niger* and *Cupriavidus***
731 ***oxalaticus* in Transwell® inserts and bronchiole-on-a-chip (BoC) devices.** (A) Control
732 showing healthy differentiated bronchial epithelial cells. (B) Bronchial epithelial cells infected
733 with *A. niger*. (C) LDH leakage was measured as a proxy for cell damage. In the presence of
734 the fungus, no LDH has been detected, probably because of the destruction of the tissue by *A.*
735 *niger* (B). *C. oxalaticus* cause significantly more LDH leakage that the basal LDH level of
736 control cells (p-value = 0,004). C: lung cells; C+F: lung cells + fungus; C+B: lung cells +
737 bacteria; C+F+B: lung cells + fungus + bacteria. For C, the results represent the mean + sd of
738 three independent measurements for the Transwell® inserts for each condition (three biological
739 replicates, n = 3). LDH results for the BoC devices represents the mean + sd of three
740 measurements per condition (one replicate, n = 1).